
An adversarial algorithm for variational inference with a new role for acetylcholine

Ari S. Benjamin & Konrad P. Kording

Department of Bioengineering
University of Pennsylvania
Philadelphia, PA 19104
aarrii@seas.upenn.edu

Abstract

Sensory learning in the mammalian cortex has long been hypothesized to involve the objective of variational inference (VI). Likely the most well-known algorithm for cortical VI is the Wake-Sleep algorithm (Hinton et al. 1995). However Wake-Sleep problematically assumes that neural activities are independent given lower-layers during generation. Here, we construct a VI system that is both compatible with neurobiology and avoids this assumption. The core of the system is a wake-sleep discriminator that classifies network states as inferred or self-generated. Inference connections learn by opposing this discriminator. This adversarial dynamic solves a core problem within VI, which is to match the distribution of stimulus-evoked (inference) activity to that of self-generated activity. Meanwhile, generative connections learn to predict lower-level activity as in standard VI. We implement this algorithm and show that it can successfully train the approximate inference network for generative models. Our proposed algorithm makes several biological predictions that can be tested. Most importantly, it predicts a teaching signal that is remarkably similar to known properties of the cholinergic system.

1 Introduction

Variational inference is an objective for unsupervised representation learning and, for much of its long history, a hypothesis for how the sensory cortex might learn (Hinton & Sejnowski, 1983; Hinton & Ghahramani, 1997; Dayan et al., 2001). This objective specifies that feedback connections should model lower-layer activity, while feedforward connections should infer the posterior distribution of higher layers that could have generated lower layers. The appeal of the VI hypothesis stems from several distinct perspectives, each of which is supported by an extensive literature. Principal among these are analysis-by-synthesis theories of perception, efficient coding, and predictive processing.

Analysis-by-synthesis holds that human perceptions reflect inferences of the causes that could have led to sensory data, rather than the data itself (Yuille & Kersten, 2006; Mumford, 1994). This perception-as-inference view has experimental support from both perceptual studies (e.g. Kording et al. (2007); Kleinschmidt & Jaeger (2015); Dasgupta et al. (2020)) and neurophysiological studies (Berkes et al., 2011). Instead of defining causes as objective things in the world, analysis-by-synthesis goes further to state that causes and the way they relate to inputs must be learned as well through some internal generative model. Variational inference is a strategy to train both the inference and generative models of an analysis-by-synthesis system (Hinton & Sejnowski, 1983).

Variational inference is also a way to create a representational code for inputs in which the average number of bits required to communicate the neural state is as small as possible (Hinton & Zemel, 1994). The idea of efficient neural coding predated variational inference (Barlow et al., 1961), but since the 1990's a number of studies have argued that neural representations are indeed efficient

in this sense (Rieke et al., 1995; Olshausen & Field, 1996; Bell & Sejnowski, 1997; Vinje, 2002; Weliky et al., 2003; Harper & McAlpine, 2004). The way VI achieves efficient representations is with the generative connections; only the bits representing error between feedback predictions and stimulus-driven, bottom-up activities need be communicated (Hinton et al., 1995).

Finally, there is now great interest in the idea that feedback connections represent predictions of lower layers (Keller & Mrsic-Flogel, 2018). Compelling instances of predictive processing are those situations in which neurons that respond classically to one sensory domain, such as sound, develop dependencies upon cross-modal signals that are generally predictive, such as muscle activity (Fiser et al. (2016); Schneider et al. (2018); Attinger et al. (2017)). Variational inference provides one strategy by which predictive feedback connections could be learned.

Despite the interest from these interrelated perspectives, it is still unclear whether the cortex actually learns via VI. What is missing is a mechanistic explanation of how this objective is attained through a biologically implemented algorithm.

The Wake-Sleep (WS) algorithm is perhaps the best-known example of an algorithm for variational inference in multilayer networks that is biologically plausible (Hinton et al., 1995). To sample from the generated distribution, WS introduces an offline, ‘fantasizing’ phase. During this phase the inference connections learn by trying to predict the higher-layer activity that generated lower layer activity. However, this strategy assumes that neurons fire independently given the lower-layer activity they generated. This assumption is not in general correct and ignores ‘explaining away’ phenomena. While many other algorithms for variational inference have been introduced that address problems with WS (Mnih & Gregor, 2014; Paisley et al., 2012; Bornschein & Bengio, 2014; Kingma & Welling, 2013; Rezende et al., 2014), it is controversial how the brain might implement these algorithms.

Since VI requires that neural activity during the inference phase should have the same distribution as in the generating phase, we suggest in this work that these distributions could be matched adversarially. Like the Wake-Sleep algorithm, this algorithm would operate in alternating online and offline phases. In addition to a network with bottom-up and top-down connections, there would be a second population whose role is to classify activity as inferred or generated. The inference connections change to trick this discriminator, while the generative connections maximize the log-likelihood of lower layers given higher layers during inference. We call this the Adversarial Wake-Sleep algorithm.

We then argue that a biological implementation of the wake-sleep discriminator would look similar to the cholinergic system. In addition to being anatomically similar to what would be required, projecting across the sensory cortex (Liu et al., 2015), acetylcholine has profound effects on representation learning in the critical period of development (Kilgard & Merzenich, 1998). Like acetylcholine, the wake-sleep discriminator’s output broadly resembles unfamiliarity and uncertainty about causes (Yu & Dayan, 2005). This theory does not explain all of acetylcholine’s varied effects, which range from attention to stress, but we find it plausible enough to merit closer scrutiny. We suggest an experiment that could test the interpretation.

2 Preliminaries

2.1 Setting and notation

We consider a noisy multilayer neural network whose hidden state at each layer we denote as the vector h_i . In the current work we only consider networks without skip connections. We define the inference network \mathcal{F} as a set of *feedforward* edges from lower layers to higher layers. The edges in \mathcal{F} define a conditional probability distribution over hidden states, $p(h|x; \mathcal{F})$.

We also define a set of *feedback* edges from higher layers to lower layers. These define the generative network \mathcal{G} . When the top layer h_N is set to a particular value (a sample from some fixed prior), the edges in \mathcal{G} define the conditional distribution over the lower layers and input $p(x, h_{1:N-1}|h_N; \mathcal{G})$. Note while \mathcal{F} and \mathcal{G} are different networks, they are both directed sets of edges on the same nodes.

The algorithm is general to discrete and continuous h_i , as well as to the form of noise injected into all h_i in both inference and generation. In applications where backpropagation will be used, we are restricted to continuous latent variables and reparameterizable noise families.

2.2 Background: variational inference

The goal of VI is to obtain a generative model for which observations are ‘minimally surprising’, in the sense that the model maximizes the average log-likelihood of the data:

$$\mathcal{L}(\mathcal{G}) \equiv \mathbb{E}_{x \sim p(x)}[\mathcal{L}(x, \mathcal{G})] = \mathbb{E}_{x \sim p(x)}[\log p(x; \mathcal{G})].$$

This is equivalent to obtaining a generative model that minimizes $\text{KL}(p(x) \| p(x; \mathcal{G}))$, the Kullback-Leibler divergence between the actual and generated distributions over inputs. Directly evaluating this objective problematically requires marginalizing over all hidden states: $p(x; \mathcal{G}) = \int dh p(x, h; \mathcal{G})$.

VI uses the inference model \mathcal{F} to train \mathcal{G} despite this central difficulty (see Dayan et al. (2001); Bishop (2006); MacKay (2003) for introduction). The inference model is meant to approximate the "inverse" of \mathcal{G} , in the sense that $p(h|x; \mathcal{F})$ should approximate the posterior $p(h|x; \mathcal{G})$ for any x in $p(x)$. The combined objective that \mathcal{F} and \mathcal{G} must maximize is:

$$\mathcal{L}(x, \mathcal{G})_{ELBO} = \mathbb{E}_{h \sim p(h|x; \mathcal{F})} \left[\log \frac{p(x, h; \mathcal{G})}{p(h|x; \mathcal{F})} \right].$$

This expression is often called the evidence lower-bound (ELBO) because it can be written as:

$$\mathcal{L}(x, \mathcal{G})_{ELBO} = \mathcal{L}(x, \mathcal{G}) - \text{KL}(p(h|x; \mathcal{F}) \| p(h|x; \mathcal{G})). \quad (1)$$

$\mathcal{L}(x, \mathcal{G})_{ELBO}$ is a lower bound to $\mathcal{L}(x, \mathcal{G})$. The negative of the ELBO is also sometimes called the ‘variational free energy’ due its alternative expression as the inference distribution’s energy (under the generative model) minus its entropy:

$$-\mathcal{L}(x, \mathcal{G})_{ELBO} = \mathbb{E}_{h \sim p(h|x; \mathcal{F})} \left[-\log p(x, h; \mathcal{G}) \right] - H(p(h|x; \mathcal{F})).$$

Training \mathcal{G} to maximize $\mathcal{L}(\mathcal{G})_{ELBO}$ is straightforward (given \mathcal{F}) in a multilayer network. At each layer h_i the generative connections change to maximize the log-likelihood of lower layers given upper layers. For later reference we define this layerwise objective as U :

$$U(\mathcal{F}, \mathcal{G}) = \mathbb{E}_{x \sim p(x)} \mathbb{E}_{h \sim p(h|x; \mathcal{F})} \left[\log p(x|h_1; \mathcal{G}) + \sum_i^{N-1} \log p(h_i|h_{i+1}; \mathcal{G}) \right] \quad (2)$$

As we discuss further in Section 6, this update rule is local and biologically plausible.

3 Adversarial Wake-Sleep

3.1 Variational inference as distribution matching

Relative to the ease of training \mathcal{G} , it is a much harder subproblem to train \mathcal{F} given \mathcal{G} . There are two main approaches the VI literature. The first is to try to calculate the gradient of $\mathcal{L}(x, \mathcal{G})_{ELBO}$ directly with respect to \mathcal{F} . This is possible but requires reducing the variance through control-variate techniques (Paisley et al., 2012; Mnih & Gregor, 2014) or reparameterization of the expectations over h (Kingma & Welling, 2013; Rezende et al., 2014). The key characteristic of this strategy is that it is performed online and does not require an offline, purely generative "Sleep" phase. This is one possible strategy as to how the cortex might implement VI (Rezende & Gerstner, 2014).

An alternative approach to VI uses alternating online and offline phases. As noted by the Wake-Sleep algorithm, one can easily ‘fantasize’ samples from the *joint* distribution $p(x, h; \mathcal{G})$ by choosing the top layer from the prior $p(h_N)$ and propagating through the rest of the network. Instead of matching the generative posterior for a particular sample, we can instead match the joint distributions $p(x, h; \mathcal{F})$ and $p(x, h; \mathcal{G})$. If these can be matched, all marginals and conditionals will be matched as well.

To see the equivalence of these objectives, consider the expectation of the ELBO over $p(x)$:

$$\mathcal{L}(\mathcal{G})_{ELBO} \equiv \mathbb{E}_{x \sim p(x)}[\mathcal{L}(x, \mathcal{G})_{ELBO}] = \mathbb{E}_{x \sim p(x)} \mathbb{E}_{h \sim p(h|x; \mathcal{F})} \left[\log \frac{p(x, h; \mathcal{G})}{p(h|x; \mathcal{F})} \right].$$

To this expression let us add the entropy of the data $H[x] = -\mathbb{E}_{x \sim p(x)}[\log p(x)]$, which does not depend on \mathcal{F} or \mathcal{G} . Incorporating this into the expectations in $\mathcal{L}(\mathcal{G})_{ELBO}$, and for convenience denoting the joint distribution of real x and inferred h as $p(x, h; \mathcal{F})$, we obtain a new objective with same stationary points for \mathcal{F} and \mathcal{G} that is the KL divergence between the joint distributions:

$$\mathcal{L}(\mathcal{G})_{joint} = \mathbb{E}_{x, h \sim p(x, h; \mathcal{F})} \left[\log \frac{p(x, h; \mathcal{G})}{p(x, h; \mathcal{F})} \right].$$

3.2 An adversarial wake-sleep strategy for matching the joint distributions

Our proposal is to match $p(x, h; \mathcal{F})$ and $p(x, h; \mathcal{G})$ adversarially. We introduce a discriminator, or series of discriminators, that sees the entire network state. The discriminator tries to classify the state as inference-like or generative-like, and the inference network (but not the generative network) changes to trick it. Generative connections maximize the log-likelihood of lower layers (Eq. 2).

The discriminator, which we denote as \mathcal{D} , maps the state (x, h_1, \dots, h_N) to a single value. The objective upon \mathcal{D} depends on which notion of distance between distributions one would like to minimize. VI requires minimizing the KL divergence between $p(x, h; \mathcal{F})$ and $p(x, h; \mathcal{G})$. However, given the fragility of adversarial learning, we argue one should choose a metric that better facilitates training. Here we take the Wasserstein GAN formulation and minimize the Wasserstein-1 distance between the inference and generative joint distributions (Arjovsky et al., 2017). In this case, \mathcal{D} simply tries to increase its output during inference and decrease it during generation. Its overall objective is:

$$V(\mathcal{F}, \mathcal{G}, \mathcal{D}) = \mathbb{E}_{(x, h) \sim p(x, h; \mathcal{F})} [\mathcal{D}(x, h)] - \mathbb{E}_{(x, h) \sim p(x, h; \mathcal{G})} [\mathcal{D}(x, h)]. \quad (3)$$

An additional constraint upon \mathcal{D} in a Wasserstein GAN (WGAN) is that it is 1-Lipschitz continuous; in experiments we apply a gradient penalty throughout learning (Gulrajani et al., 2017).

While the discriminator maximizes this objective, the inference connections minimize it. This is to say that \mathcal{F} minimizes the output of \mathcal{D} during inference, $\mathbb{E}_{(x, h) \sim p(x, h; \mathcal{F})} [\mathcal{D}(x, h)]$.

As in the original Wake-Sleep algorithm, the above objectives can be calculated and optimized in two separate phases. In the online phase, a batch of examples are run through the inference network to obtain samples of h from $p(x, h; \mathcal{F})$, \mathcal{G} is updated to predict lower layers, and \mathcal{D} and \mathcal{F} are updated to maximize or minimize the output of \mathcal{D} . In the offline phase, samples are ‘fantasized’ from $p(x, h; \mathcal{G})$, and \mathcal{D} learns to decrease its output. We present the step-by-step algorithm in the Appendix.

3.2.1 Reducing the input dimension for \mathcal{D}

In the formulation above, the discriminator has an input dimension equal to the entire space of activations of the network. This can be decreased by taking into account the structure of the network on which \mathcal{F} and \mathcal{G} are defined. If this network has no skip connections, \mathcal{F} and \mathcal{G} define a Markov chain of layer transformations. The joint probability distribution can be factored by layer:

$$\begin{aligned} p(x, h_0, h_1, \dots, h_N, \mathcal{F}) &= p(h_N | h_{N-1}; \mathcal{F}) p(h_{N-1} | h_{N-2}; \mathcal{F}) \dots p(h_1 | x; \mathcal{F}) p(x) \\ p(x, h_0, h_1, \dots, h_N, \mathcal{G}) &= p(x | h_1; \mathcal{G}) p(h_1 | h_2; \mathcal{G}) \dots p(h_{N-1} | h_N; \mathcal{G}) p(h_N; \mathcal{G}) \end{aligned}$$

If the joint distributions between every two layers $p(h_i, h_{i+1})$ are matched between inference and generation, each factored conditional will be matched as well. Thus, as displayed in Figure 1, a separate sub-discriminator \mathcal{D}_i can be used for each pair of layers. The dimensionality of the inputs of each \mathcal{D}_i scales with the width of the network but not its depth.

3.2.2 Application to discrete hidden states

Suppose the units in the neural network can take one of a few discrete values, such as for the binary on-or-off neurons in a Helmholtz machine and the original Wake-Sleep algorithm. In this case one cannot take the derivative of \mathcal{D} with respect to the inference weights. Instead, we can apply the trick of REINFORCE (Williams, 1992). The gradient of $\mathbb{E}_{h \sim p(h|x; \mathcal{F})} [\mathcal{D}(x, h)]$ with respect to the parameters at layer i becomes:

$$\mathbb{E}_{h \sim p(h|x; \mathcal{F})} [\mathcal{D}(x, h) \nabla_{\mathcal{F}} \log p(h_{i+1} | h_i; \mathcal{F})] \quad (4)$$

This is exactly analogous to REINFORCE but with the discriminator replacing reward. To be usable in large networks, however, the variance of this estimator would have to be reduced considerably.

4 Experiments

We tested several implementations to explore when Adversarial Wake-Sleep works and when it could be beneficial in generative modeling. Overall, we found that when applied as the sole learning objective, the algorithm works but is quite fragile to optimization and stabilization methods. However, it is easily stabilized by adding other unsupervised objectives beyond VI.

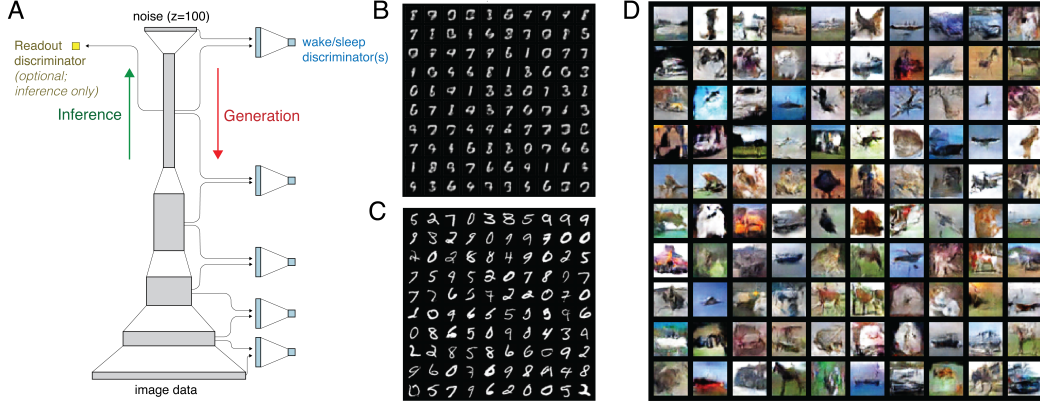


Figure 1: Generating images on a DCGAN architecture with Adversarial Wake-Sleep. A) Basic architecture. Images are passed up, or noise is passed down, the convolutional architecture. Dense 2-layer wake-sleep discriminators read out from pairs of layers in either stage. Optionally, generated images can be passed up and a readout discriminator estimates whether the top layer was induced by a real or generated image (Section 4.2) B) MNIST digits generated by standard Adversarial Wake-Sleep, in which generative connections learn only by maximizing the likelihood of lower-level inference activations. C) Adding the readout discriminator allows much better generation. Here the GAN/VI interpolation parameter was set to $\gamma = 0.999$. D) CIFAR-10 generation with $\gamma = 0.9$.

4.1 Adversarial wake-sleep as the sole objective

We tested the algorithm at training a DCGAN (Radford et al., 2015) to generate 32x32 MNIST digits and CIFAR-10 images (Figure 1). This is a full-convolutional, 5 layer network with ReLU activations to which we add isotropic Gaussian noise. Additional training details can be found in the Appendix.

As a point of comparison, the original Wake-Sleep algorithm did not converge to produce digits in this continuous setting with Gaussian noise models (32x32 MNIST digits, continuous-valued pixels and ReLU activations), even despite extensive experiments (as detailed in the Appendix). This was not because of the convolutional operators, as WS did produce digit-like images on a stochastic binary Helmholtz machine in a DCGAN-like configuration.

Adversarial Wake-Sleep does produce digits on 32x32 MNIST (Fig. 1B). This serves as a basic proof of concept for its feasibility. However, we found the algorithm to be quite unstable and as a result the generated images are far from state-of-the-art in diversity and quality. The most common type of failure was mode collapse in the inference network, which then prevented the generator from learning successfully (see Appendix for an example). We found that popular stabilization tricks in \mathcal{F} and \mathcal{G} were essential. The local divisive normalization operator of Karras et al. (2017), for example, greatly helped stabilize training. Incidentally, divisive normalization has long been known to be implemented in the sensory cortex (Heeger, 1992). If this algorithm is implemented in the cortex, it is likely that other properties of cortical networks act to stabilize training, as well.

4.2 Reusing the inference network as a discriminator

Adversarial Wake-Sleep can be stabilized with a small architectural addition: a linear readout from the top layer. The role of this *readout discriminator* \mathcal{R} is to determine whether the inference network has processed a real image or a generated image.

This addition preserves the architecture and generative goal but modifies the approach. In addition to maximizing the log-likelihood of lower inference layers, the generator now also tries to produce images that the readout discriminator classifies as real. This requires modifying the Sleep phase such that generated images are passed back up through the inference network. The inference network, in addition to its Adversarial Wake-Sleep objective, also now helps the readout discriminator by trying to map real and generated images to linearly separable subspaces.

The idea that an inference network can also serve as a discriminator on images precedes this paper (Ulyanov et al., 2018; Brock et al., 2016). However, here the inference network maps to the entire generative network state that might have led to an image, not just the top-level latent state $z = h_N$. The idea can be imagined as a GAN in which the discriminator also specifies, approximately, the posterior distribution over generative activities.

One perspective that can help understand why mixing GAN and VI objectives might work is an energy-based perspective, in analogy to learning with Contrastive Divergence (Hinton, 2002). By attempting to treat generated and real samples as differently as possible (in the eyes of \mathcal{R}) while also lowering the energy of real samples, \mathcal{R} causes \mathcal{F} to effectively raise the energy of generated samples.

This approach is precisely a simple addition of a VI and GAN objective, and might be called Doubly Adversarial Wake-Sleep. We will write the GAN objective in the WGAN form:

$$W(\mathcal{F}, \mathcal{G}, \mathcal{R}) = \mathbb{E}_{x \sim p(x)} [\mathbb{E}_{h_{N-1} \sim p(h_{N-1}|x; \mathcal{F})} \mathcal{R}(h_{N-1})] - \mathbb{E}_{x \sim p(x; \mathcal{G})} [\mathbb{E}_{h_{N-1} \sim p(h_{N-1}|x; \mathcal{F})} \mathcal{R}(h_{N-1})]. \quad (5)$$

Let γ be a hyperparameter that controls the relative influence of the VI or GAN objectives, with a value of 1 being pure Adversarial Wake-Sleep and 0 being a GAN. Then the overall objectives are:

$$\begin{aligned} \mathcal{G} &= \min_{\mathcal{G}} \left[-\gamma U(\mathcal{F}, \mathcal{G}) + (1 - \gamma) W(\mathcal{F}, \mathcal{G}, \mathcal{R}) \right] \\ \mathcal{F} &= \min_{\mathcal{F}} \left[\gamma V(\mathcal{F}, \mathcal{G}, \mathcal{D}) - (1 - \gamma) W(\mathcal{F}, \mathcal{G}, \mathcal{R}) \right] \\ \mathcal{D}, \mathcal{R} &= \max_{\mathcal{D}, \mathcal{R}} [\gamma V(\mathcal{F}, \mathcal{G}, \mathcal{D}) + (1 - \gamma) W(\mathcal{F}, \mathcal{G}, \mathcal{R})] \end{aligned}$$

This addition stabilized Adversarial Wake-Sleep to competitive levels while still preserving a biologically plausible architecture and wake-sleep dynamic. When trained on MNIST and CIFAR-10, the algorithm generates images of good quality (Fig. 2C, D).

4.2.1 The effect of varying γ

In Figure 2 we train a DCGAN to generate CIFAR-10 images while interpolating between the GAN and VI objectives using γ . Relative to a standard WGAN-GP ($\gamma = 0$), adding the inference requirement to the discriminator does not harm generative performance. As measured by the FID score (Heusel et al., 2017), the quality of generated images remains high (Fig. 2B). Furthermore, increasing γ progressively introduces the required layerwise autoencoding relationship, as can be seen by passing test images up one layer of \mathcal{F} and back down one layer of \mathcal{G} and calculating the reconstruction error (Fig. 2A). These results show that a single feedforward network can learn to be a (variational) inference network while still being useful as a discriminator.

5 Related work in generative modeling

Several generative modeling papers have approached representation learning by adversarially matching joint distributions of latent vectors and inputs. Both the Adversarial Variational Inference (ALI) and BiGAN algorithms propose a third network that discriminates between the paired data and inferred latents (x, \hat{z}) from the latents and the data they generated (\hat{x}, z) , and train the generator and inference network to trick this discriminator (Donahue et al. (2016); Dumoulin et al. (2016)). This approach has been extended in various ways (Pu et al., 2017; Srivastava et al., 2017; Donahue & Simonyan, 2019). This setting differs from ours in that the latent vector z is not the vector of activations of the entire generator/inference network, but the noise vector that the generator takes as input. This means that generative connections cannot be trained to predict lower-layer activations, as in VI; in ALI and BiGAN all weight changes are due to gradients that pass through the discriminator.

A step towards our algorithm are the hierarchical approaches of Belghazi et al. (2018) and Huang et al. (2017). Unlike ALI and BiGAN, the latent vector is multileveled; separate discriminators match the latent vector’s distribution at every level of hierarchy. However, in these algorithms the generator network trains against the discriminator and not in a layerwise maximum-likelihood fashion.

The idea of re-using the discriminator in a GAN as the inference network has also been proposed in several variants (Brock et al., 2016; Ulyanov et al., 2018; Huang et al., 2018; Munjal et al., 2019;

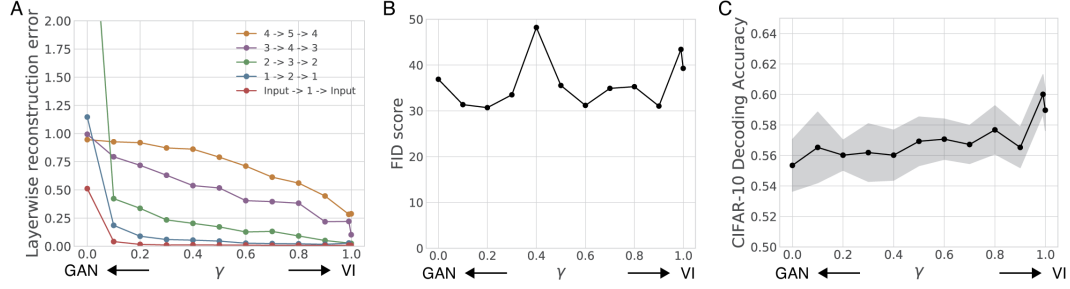


Figure 2: Interpolating between a GAN and VI objective, and in doing so incrementally turning the discriminator into an approximate inference network. The network is a DCGAN architecture trained to generate CIFAR-10 images, and all runs are with the random seed set to 0. A) Increasing γ makes the discriminator more like an inference network; here measured by the error between each inference layer and the generative prediction after passing up one layer, for CIFAR-10 test images. B) Increasing γ does not harm the generated images quality and diversity as measured by the FID score. The highest two values shown are $\gamma = 0.99, 0.999$. C) The linear decodability of class labels from layer 4 of the inference network’s as measured with a linear SVM trained with 10-fold crossvalidation on the test set. The envelope represents the standard deviation across folds.

Bang et al., 2020). These studies show that a GAN can be made into an autoencoder by pairing the discriminator and generator end-to-end and applying reconstruction costs. Our result is again different in that the inference network maps to the posterior of the entire generative network state rather than the top-level noise vector, allowing the maximum-likelihood update.

6 Potential biological implementation

The overall architecture of our biological model is shown schematically in Figure 3. There are two key elements: the discriminator, and how the generative model learns.

6.1 Learning the feedback connections

In VI, the generative connections change to better predict lower-level activity given upper layers. A biological neuron implementing this rule would need an additional compartment to integrate feedback activity so it could compare that prediction to the feedforward-driven somatic activity. This ‘dendritic prediction of somatic activity’ has in fact been proposed as an explanation of how spike-timing dependent plasticity depends on postsynaptic voltage (Urbanczik & Senn, 2014). It should be remarked that this rule is not enough to learn to model lower layers; for this the feedforward activity needs to match the generative posterior. This is the purpose of the discriminator.

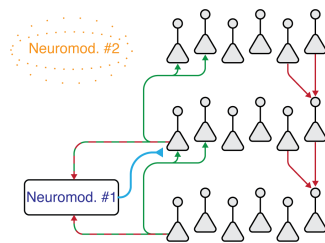


Figure 3: A biological implementation. During ‘Wake’, feed-forward connections drive somatic activity. Feedback connections synapse on a segregated dendritic compartment and their synapses change so the compartment better predicts somatic activity. Connections to the wake/sleep discriminator (Neuromod. #1, putatively ACh) change to increase its activity, and Neuromod. #1 is projected back to gate feedforward plasticity. During ‘Sleep’, feedback connections drive somatic activity, and the wake/sleep discriminator tries to decrease its activity. The scheme requires a second neuromodulator (#2) released in ‘Sleep’ that controls whether feedforward or feedback connections drive somatic activity.

6.2 Is the cholinergic system a wake-sleep discriminator?

Our algorithm requires a non-cortical region that projects across the sensory cortex that has the ability to gate or modulate plasticity, especially within the critical period of development. This led us to speculate that the cholinergic system could play this role. We found that a number of other features of acetylcholine are consistent with this interpretation, as well.

One of the many interpretations of acetylcholine (ACh) is that it signals unfamiliarity and uncertainty. In the work of Yu and Dayan, ACh signals the uncertainty about top-down, contextual information in sensory processing tasks (Dayan & Yu, 2002; Yu & Dayan, 2002). This hypothesis was later narrowed to a signal of expected, or learned, uncertainty (in contrast to unexpected uncertainty, or surprise) (Yu & Dayan, 2005). This is very close to how a discriminator would appear to respond in the ‘Wake’ phase. The discriminator is a learned estimate of whether a network state could have been self-generated. This means that the discriminator has high activity when it estimates that the inference network failed to produce high-level activity that could explain away the lower-level activity via the generative connections.

Another canonical feature of ACh is its control over cortical plasticity (Gu, 2002; Rasmusson, 2000). During the critical period in which sensory representations are formed, the cortex may irreversibly learn to respond to only one eye if the other is closed. However, if ACh is prevented from being released (Bear & Singer, 1986), or if its effect upon somatostatin-positive interneurons is blocked (Yaeger et al., 2019), cortical remapping is impaired. Conversely, and even after the critical period has ended, one can artificially induce profound changes in cortical representations by pairing ACh release with sensory stimuli (Kilgard & Merzenich, 1998). These findings have been replicated across many sensory domains (Gu, 2002) and indicate that ACh has a crucial role in the cortex’s strategy for learning sensory representations.

Acetylcholine is largely released during waking experience and in comparable amounts during REM sleep, but in low amounts in other stages of sleep (Kametani & Kawamura, 1990). This would be expected if ACh played a role as a wake-(REM)sleep discriminator, but is harder to explain with interpretations that stop at attention and unfamiliarity. It is worth noting that ACh is implicated in the control of sleep as well (Ozen Irmak & de Lecea, 2014; Hobson et al., 1975).

Acetylcholine has an extraordinary number of functions within the nervous system, and we do not imagine that this new interpretation should consolidate them all. Its role in attention, for example, appears difficult to explain in any rigorous way as relating to a wake-sleep discriminator (Sarter et al., 2005). Nevertheless, we believe this conjunction of sensory uncertainty, representation learning, and sleep is remarkably consistent with what would be required of a wake-sleep discriminator for VI.

6.3 Predictions

Adversarial Wake-Sleep could be tested for in the following manner. During the critical period of sensory learning, one could selectively silence activity during the stage of sleep most likely to correspond to the offline, generative phase in this algorithm (most plausibly REM sleep). This affects the generative distribution. One could then observe if waking activity changes, via apparently experience-dependent plasticity, to match that perturbed distribution. If so, one could further ask whether ACh mediates that change.

7 Discussion

If variational inference acts as the sensory cortex’s learning objective, or at least some part of it, the cortex could learn the inference connections with an adversarial strategy. It requires a wake-sleep discriminator, which has the simple objective of increasing its output during a stage of sleep and decreasing its output during wake. This objective is easier to learn for a biological area than directly estimating the variational free energy of the entire sensory cortex, as would be required if this strategy were not used (Mnih & Gregor, 2014; Rezende & Gerstner, 2014). This adversarial concept may help to understand the role of acetylcholine in learning, pending further experiments.

Our experiments showed that Adversarial Wake-Sleep works to some degree but still falls far short of benchmarks in generative modeling. Other features of real cortical networks beyond divisive normalization may be required to stabilize the algorithm to competitive levels. We found one way to

improve Adversarial Wake-Sleep was to re-use the inference network as a discriminator on inputs. We are agnostic as to whether biology takes this particular strategy, but note that it at least requires no additional architecture beyond a linear readout. This change is also consistent with a recent proposal that human perception corresponds to the processing of a discriminator (Gershman, 2019). However, we are not aware of any biological evidence that this fix is one that the cortex uses.

Our model of sensory learning is abstract. In addition to the usual differences between ANNs and biological neurons, we have not attempted to include any of the great amount that is known about sleep, the role of hippocampus in sensory learning, or a number of other potentially relevant systems.

Some of these details may answer important computational questions. For example, how do spiking neurons calculate their gradient with respect to the discriminator when given only its output? This problem is equivalent to the credit assignment problem in, for example, reinforcement learning. In our case the answer may lie in local microcircuits, and the fact the acetylcholine mediates learning largely through disinhibition (Yaeger et al., 2019). Alternatively, due to a connection between backpropagation and variational autoencoders, there is the possibility that the feedforward and feedback connections themselves could be used for the credit assignment problem (Bengio, 2014).

8 Code availability

The Pytorch code implementing this algorithm that was used for the figures in this manuscript can be found at <https://github.com/KordingLab/adversarial-wake-sleep>.

References

- Arjovsky, Martin, Chintala, Soumith, and Bottou, Léon. Wasserstein gan. *arXiv preprint arXiv:1701.07875*, 2017.
- Attinger, Alexander, Wang, Bo, and Keller, Georg B. Visuomotor Coupling Shapes the Functional Development of Mouse Visual Cortex. *Cell*, 2017. ISSN 10974172. doi: 10.1016/j.cell.2017.05.023.
- Bang, Duhyeon, Kang, Seoungyoon, and Shim, Hyunjung. Discriminator feature-based inference by recycling the discriminator of gans. *International Journal of Computer Vision*, pp. 1–23, 2020.
- Barlow, Horace B et al. Possible principles underlying the transformation of sensory messages. *Sensory communication*, 1:217–234, 1961.
- Bear, Mark F. and Singer, Wolf. Modulation of visual cortical plasticity by acetylcholine and noradrenaline. *Nature*, 320(6058):172–176, 1986. ISSN 00280836. doi: 10.1038/320172a0.
- Belghazi, Mohamed Ishmael, Rajeswar, Sai, Mastropietro, Olivier, Rostamzadeh, Negar, Mitrovic, Jovana, and Courville, Aaron. Hierarchical adversarially learned inference. *arXiv preprint arXiv:1802.01071*, 2018.
- Bell, Anthony J and Sejnowski, Terrence J. The “independent components” of natural scenes are edge filters. *Vision research*, 37(23):3327–3338, 1997.
- Bengio, Yoshua. How auto-encoders could provide credit assignment in deep networks via target propagation. *arXiv preprint arXiv:1407.7906*, 2014.
- Berkes, Pietro, Orbán, Gergo, Lengyel, Máté, and Fiser, József. Spontaneous cortical activity reveals hallmarks of an optimal internal model of the environment. *Science*, 331(6013):83–87, 2011. ISSN 00368075. doi: 10.1126/science.1195870.
- Bishop, Christopher M. *Pattern recognition and machine learning*. springer, 2006.
- Bornschein, Jörg and Bengio, Yoshua. Reweighted wake-sleep. *arXiv preprint arXiv:1406.2751*, 2014.
- Brock, Andrew, Lim, Theodore, Ritchie, James M, and Weston, Nick. Neural photo editing with introspective adversarial networks. *arXiv preprint arXiv:1609.07093*, 2016.

- Dasgupta, Ishita, Schulz, Eric, Tenenbaum, Joshua B, and Gershman, Samuel J. A theory of learning to infer. *Psychological Review*, 127(3):412, 2020.
- Dayan, Peter and Yu, Angela. Ach, uncertainty, and cortical inference. In *Advances in neural information processing systems*, pp. 189–196, 2002.
- Dayan, Peter, Abbott, Laurence F, et al. *Theoretical neuroscience*, volume 806. Cambridge, MA: MIT Press, 2001.
- Donahue, Jeff and Simonyan, Karen. Large scale adversarial representation learning. In *Advances in Neural Information Processing Systems*, pp. 10541–10551, 2019.
- Donahue, Jeff, Krähenbühl, Philipp, and Darrell, Trevor. Adversarial feature learning. *arXiv preprint arXiv:1605.09782*, 2016.
- Dumoulin, Vincent, Belghazi, Ishmael, Poole, Ben, Mastropietro, Olivier, Lamb, Alex, Arjovsky, Martin, and Courville, Aaron. Adversarially learned inference. *arXiv preprint arXiv:1606.00704*, 2016.
- Fiser, Aris, Mahringer, David, Oyibo, Hassana K., Petersen, Anders V., Leinweber, Marcus, and Keller, Georg B. Experience-dependent spatial expectations in mouse visual cortex. *Nature Neuroscience*, 19(12):1658–1664, 2016. ISSN 15461726. doi: 10.1038/nn.4385.
- Gershman, Samuel Joseph. The generative adversarial brain. *Frontiers in Artificial Intelligence*, 2:18, 2019.
- Gu, Q. Neuromodulatory transmitter systems in the cortex and their role in cortical plasticity. *Neuroscience*, 111(4):815–835, 2002. ISSN 03064522. doi: 10.1016/S0306-4522(02)00026-X.
- Gulrajani, Ishaan, Ahmed, Faruk, Arjovsky, Martin, Dumoulin, Vincent, and Courville, Aaron C. Improved training of wasserstein gans. In *Advances in neural information processing systems*, pp. 5767–5777, 2017.
- Harper, Nicol S and McAlpine, David. Optimal neural population coding of an auditory spatial cue. *Nature*, 430(7000):682, 2004.
- Heeger, David J. Normalization of cell responses in cat striate cortex. *Visual neuroscience*, 9(2): 181–197, 1992.
- Heusel, Martin, Ramsauer, Hubert, Unterthiner, Thomas, Nessler, Bernhard, and Hochreiter, Sepp. Gans trained by a two time-scale update rule converge to a local nash equilibrium. In *Advances in neural information processing systems*, pp. 6626–6637, 2017.
- Hinton, Geoffrey E. Training products of experts by minimizing contrastive divergence. *Neural computation*, 14(8):1771–1800, 2002.
- Hinton, Geoffrey E and Ghahramani, Zoubin. Generative models for discovering sparse distributed representations. *Philosophical Transactions of the Royal Society of London. Series B: Biological Sciences*, 352(1358):1177–1190, 1997.
- Hinton, Geoffrey E and Sejnowski, Terrence J. Optimal perceptual inference. In *Proceedings of the IEEE conference on Computer Vision and Pattern Recognition*, volume 448. Citeseer, 1983.
- Hinton, Geoffrey E and Zemel, Richard S. Autoencoders, minimum description length and helmholtz free energy. In *Advances in neural information processing systems*, pp. 3–10, 1994.
- Hinton, Geoffrey E, Dayan, Peter, Frey, Brendan J, and Neal, Radford M. The "wake-sleep" algorithm for unsupervised neural networks. *Science*, 268(5214):1158–1161, 1995.
- Hobson, J Allan, McCarley, Robert W, and Myzinski, Peter W. Sleep Cycle Oscillation : Reciprocal Discharge by Two Brainstem Neuronal Groups Author (s): J . Allan Hobson , Robert W . McCarley and Peter W . Wyzinski Published by : American Association for the Advancement of Science Stable URL : <http://www.jstor.or>. *Science*, 189(4196):55–58, 1975.

- Huang, Huaibo, He, Ran, Sun, Zhenan, Tan, Tieniu, et al. Introvae: Introspective variational autoencoders for photographic image synthesis. In *Advances in neural information processing systems*, pp. 52–63, 2018.
- Huang, Xun, Li, Yixuan, Poursaeed, Omid, Hopcroft, John, and Belongie, Serge. Stacked generative adversarial networks. In *Proceedings of the IEEE conference on computer vision and pattern recognition*, pp. 5077–5086, 2017.
- Ioffe, Sergey and Szegedy, Christian. Batch normalization: Accelerating deep network training by reducing internal covariate shift. *arXiv preprint arXiv:1502.03167*, 2015.
- Kametani, Hideki and Kawamura, Hiroshi. Alterations in acetylcholine release in the rat hippocampus during sleep-wakefulness detected by intracerebral dialysis. *Life sciences*, 47(5):421–426, 1990.
- Karras, Tero, Aila, Timo, Laine, Samuli, and Lehtinen, Jaakko. Progressive growing of gans for improved quality, stability, and variation. *arXiv preprint arXiv:1710.10196*, 2017.
- Keller, Georg B. and Mrcic-Flogel, Thomas D. Predictive Processing: A Canonical Cortical Computation, 2018. ISSN 10974199.
- Kilgard, Michael P. and Merzenich, Michael M. Cortical map reorganization enabled by nucleus basalis activity. *Science*, 279(5357):1714–1718, 1998. ISSN 00368075. doi: 10.1126/science.279.5357.1714.
- Kingma, Diederik P and Welling, Max. Auto-encoding variational bayes. *arXiv preprint arXiv:1312.6114*, 2013.
- Kleinschmidt, Dave F and Jaeger, T Florian. Robust speech perception: recognize the familiar, generalize to the similar, and adapt to the novel. *Psychological review*, 122(2):148, 2015.
- Körding, Konrad P, Beierholm, Ulrik, Ma, Wei Ji, Quartz, Steven, Tenenbaum, Joshua B, and Shams, Ladan. Causal inference in multisensory perception. *PLoS one*, 2(9):e943, 2007.
- Liu, Alan King Lun, Chang, Raymond Chuen Chung, Pearce, Ronald K.B., and Gentleman, Steve M. Nucleus basalis of Meynert revisited: anatomy, history and differential involvement in Alzheimer’s and Parkinson’s disease. *Acta Neuropathologica*, 129(4):527–540, 2015. ISSN 14320533. doi: 10.1007/s00401-015-1392-5.
- MacKay, David JC. *Information theory, inference and learning algorithms*. Cambridge university press, 2003.
- Miyato, Takeru, Kataoka, Toshiki, Koyama, Masanori, and Yoshida, Yuichi. Spectral normalization for generative adversarial networks. *arXiv preprint arXiv:1802.05957*, 2018.
- Mnih, Andriy and Gregor, Karol. Neural variational inference and learning in belief networks. *arXiv preprint arXiv:1402.0030*, 2014.
- Mumford, David. Neuronal architectures for pattern-theoretic problems. *Large-scale neuronal theories of the brain*, pp. 125–152, 1994.
- Munjal, Prateek, Paul, Akanksha, and Krishnan, Narayanan C. Implicit discriminator in variational autoencoder. *arXiv preprint arXiv:1909.13062*, 2019.
- Olshausen, Bruno A and Field, David J. Emergence of simple-cell receptive field properties by learning a sparse code for natural images. *Nature*, 381(6583):607, 1996.
- Ozen Irmak, Simal and de Lecea, Luis. Basal Forebrain Cholinergic Modulation of Sleep Transitions. *Sleep*, 37(12):1941–1951, 2014. ISSN 0161-8105. doi: 10.5665/sleep.4246.
- Paisley, John, Blei, David, and Jordan, Michael. Variational bayesian inference with stochastic search. *arXiv preprint arXiv:1206.6430*, 2012.
- Pu, Yuchen, Wang, Weiyao, Henao, Ricardo, Chen, Liqun, Gan, Zhe, Li, Chunyuan, and Carin, Lawrence. Adversarial symmetric variational autoencoder. In *Advances in neural information processing systems*, pp. 4330–4339, 2017.

- Radford, Alec, Metz, Luke, and Chintala, Soumith. Unsupervised representation learning with deep convolutional generative adversarial networks. *arXiv preprint arXiv:1511.06434*, 2015.
- Rasmusson, D. D. The role of acetylcholine in cortical synaptic plasticity. *Behavioural Brain Research*, 115(2):205–218, 2000. ISSN 01664328. doi: 10.1016/S0166-4328(00)00259-X.
- Rezende, Danilo and Gerstner, Wulfram. Stochastic variational learning in recurrent spiking networks. *Frontiers in Computational Neuroscience*, 8:38, 2014. ISSN 1662-5188. doi: 10.3389/fncom.2014.00038. URL <https://www.frontiersin.org/article/10.3389/fncom.2014.00038>.
- Rezende, Danilo Jimenez, Mohamed, Shakir, and Wierstra, Daan. Stochastic backpropagation and approximate inference in deep generative models. *arXiv preprint arXiv:1401.4082*, 2014.
- Rieke, Fred, Bodnar, DA, and Bialek, William. Naturalistic stimuli increase the rate and efficiency of information transmission by primary auditory afferents. *Proceedings of the Royal Society of London. Series B: Biological Sciences*, 262(1365):259–265, 1995.
- Sarter, Martin, Hasselmo, Michael E., Bruno, John P., and Givens, Ben. Unraveling the attentional functions of cortical cholinergic inputs: Interactions between signal-driven and cognitive modulation of signal detection. *Brain Research Reviews*, 48(1):98–111, 2005. ISSN 01650173. doi: 10.1016/j.brainresrev.2004.08.006.
- Schneider, David M, Sundararajan, Janani, and Mooney, Richard. A cortical filter that learns to suppress the acoustic consequences of movement. *Nature*, 561(7723):391–395, 2018.
- Srivastava, Akash, Valkov, Lazar, Russell, Chris, Gutmann, Michael U, and Sutton, Charles. Veegan: Reducing mode collapse in gans using implicit variational learning. In *Advances in Neural Information Processing Systems*, pp. 3308–3318, 2017.
- Ulyanov, Dmitry, Vedaldi, Andrea, and Lempitsky, Victor. It takes (only) two: Adversarial generator-encoder networks. In *Thirty-Second AAAI Conference on Artificial Intelligence*, 2018.
- Urbanczik, Robert and Senn, Walter. Learning by the dendritic prediction of somatic spiking. *Neuron*, 81(3):521–528, 2014.
- Vinje, W. E. Sparse Coding and Decorrelation in Primary Visual Cortex During Natural Vision. *Science*, 287(5456):1273–1276, 2002. ISSN 00368075. doi: 10.1126/science.287.5456.1273.
- Weliky, Michael, Fiser, József O., Hunt, Ruskin H., and Wagner, David N. Coding of natural scenes in primary visual cortex. *Neuron*, 2003. ISSN 08966273. doi: 10.1016/S0896-6273(03)00022-9.
- Williams, Ronald J. Simple statistical gradient-following algorithms for connectionist reinforcement learning. *Machine learning*, 8(3-4):229–256, 1992.
- Yaeger, Courtney E., Ringach, Dario L., and Trachtenberg, Joshua T. Neuromodulatory control of localized dendritic spiking in critical period cortex. *Nature*, 56, 2019. ISSN 0028-0836. doi: 10.1038/s41586-019-0963-3. URL <http://www.nature.com/articles/s41586-019-0963-3>.
- Yu, Angela and Dayan, Peter. Acetylcholine in cortical inference. *Neural Networks*, 15(4-6):719–730, 2002.
- Yu, Angela J. and Dayan, Peter. Uncertainty, neuromodulation, and attention. *Neuron*, 2005. ISSN 08966273. doi: 10.1016/j.neuron.2005.04.026.
- Yuille, Alan and Kersten, Daniel. Vision as Bayesian inference: analysis by synthesis? *Trends in Cognitive Sciences*, 10(7):301–308, 2006. ISSN 13646613. doi: 10.1016/j.tics.2006.05.002.

Appendix

8.1 Algorithm

Algorithm 1 Adversarial Wake-Sleep

Here shown with stochastic gradient descent and WGAN-GP distribution-matching objective.

Require: $\eta_{\mathcal{F}}, \eta_{\mathcal{G}}, \eta_{\mathcal{D}}$ ▷ Learning rates
Require: $\lambda_{\mathcal{D}}$ ▷ Gradient penalty size

1: **procedure**
2: $\theta_{\mathcal{D}}, \theta_{\mathcal{F}}, \theta_{\mathcal{G}} \sim \theta_0$ ▷ Initialize parameters in \mathcal{D} , \mathcal{F} , and \mathcal{G} .
3: **while** not converged **do**
4: **Wake**
5: draw $x \sim p(x)$ ▷ Observe batch of data
6: sample $h \sim p(h|x; \mathcal{F})$ ▷ Infer hidden states
7: calculate $D = \mathcal{D}(x, h)$ ▷ Calculate discriminator's value
8: calculate $GP = \lambda_{\mathcal{D}} \|\nabla_{x,h} D - 1\|$ ▷ Calculate gradient penalty
9: $\Delta\theta_{\mathcal{D}} \leftarrow \eta_{\mathcal{D}} \nabla_{\theta_{\mathcal{D}}} (D - GP)$ ▷ \mathcal{D} attempts to increase output
10: $\Delta\theta_{\mathcal{F}} \leftarrow -\eta_{\mathcal{F}} \nabla_{\theta_{\mathcal{F}}} D$ ▷ \mathcal{F} attempts to decrease D
11: $\Delta\theta_{\mathcal{G}} \leftarrow \eta_{\mathcal{G}} \nabla_{\theta_{\mathcal{G}}} U(\mathcal{F}, \mathcal{G})$ ▷ Adjust \mathcal{G} to maximize variational log-likelihood (Eq. 2)

12: **Sleep**
13: sample $h_N \sim p(h_N; \mathcal{G})$ ▷ Sample top-level hidden state
14: calculate $(x, h) \sim p(x, h|h_N; \mathcal{G})$ ▷ Propagate through \mathcal{G}
15: calculate $D = \mathcal{D}(x, h)$ ▷ Calculate discriminator's value
16: calculate $GP = \lambda_{\mathcal{D}} \|\nabla_{x,h} D - 1\|$ ▷ Calculate gradient penalty
17: $\Delta\theta_{\mathcal{D}} \leftarrow \eta_{\mathcal{D}} \nabla_{\theta_{\mathcal{D}}} (-D - GP)$ ▷ \mathcal{D} attempts to decrease output
18: **end while**
19: **return** \mathcal{D}, \mathcal{F} , and \mathcal{G} .
20: **end procedure**

Algorithm 2 Doubly Adversarial Wake-Sleep

Require: $\eta_{\mathcal{F}}, \eta_{\mathcal{G}}, \eta_{\mathcal{D}}, \eta_{\mathcal{R}}$ ▷ Learning rates
Require: γ ▷ Interpolation parameter

1: **procedure**
2: $\theta_{\mathcal{D}}, \theta_{\mathcal{F}}, \theta_{\mathcal{G}}, \theta_{\mathcal{R}} \leftarrow \theta_0$ ▷ Initialize parameters in $\mathcal{D}, \mathcal{F}, \mathcal{R}$, and \mathcal{G} .
3: **while** not converged **do**
4: **Wake**
5: draw $X \sim p(x)$ ▷ Observe batch of data
6: sample $h \sim p(h|x; \mathcal{F})$ ▷ Infer hidden states
7: calculate $D = \mathcal{D}(x, h)$ ▷ Calculate discriminator's value
8: calculate $GP = \|\nabla_{x,h} D - 1\|$ ▷ Calculate gradient penalty
9: calculate $R = \mathcal{R}(h_{N-1})$ ▷ Calculate readout discriminator's value
10: $\Delta\theta_{\mathcal{D}} \leftarrow \eta_{\mathcal{D}} \nabla_{\theta_{\mathcal{D}}} \gamma(D - GP)$ ▷ \mathcal{D} attempts to increase output
11: $\Delta\theta_{\mathcal{F}} \leftarrow -\eta_{\mathcal{F}} \nabla_{\theta_{\mathcal{F}}} (\gamma D + (1 - \gamma)R)$ ▷ \mathcal{F} attempts to decrease D and increase R
12: $\Delta\theta_{\mathcal{G}} \leftarrow \eta_{\mathcal{G}} \nabla_{\theta_{\mathcal{G}}} \gamma U(\mathcal{F}, \mathcal{G})$ ▷ Adjust \mathcal{G} to maximize variational log-likelihood (Eq. 2).
13: $\Delta\theta_{\mathcal{R}} \leftarrow \eta_{\mathcal{R}} \nabla_{\theta_{\mathcal{R}}} (1 - \gamma)R$ ▷ \mathcal{R} attempts to increase output

14: **Sleep**
15: sample $h_N \sim p(h_N; \mathcal{G})$ ▷ Sample top-level hidden state
16: calculate $(\hat{x}, h) \sim p(x, h|h_N; \mathcal{G})$ ▷ Propagate through \mathcal{G}
17: calculate $D = \mathcal{D}(\hat{x}, h)$ ▷ Calculate discriminator's value
18: calculate $h_{N-1} \sim p(h_{N-1}|\hat{x}; \mathcal{F})$ ▷ Pass generated samples back up through \mathcal{F}
19: calculate $R = \mathcal{R}(h_{N-1})$ ▷ Calculate readout discriminator
20: calculate $GP = \|\nabla_{x,h} D - 1\|$ ▷ Calculate gradient penalty
21: $\Delta\theta_{\mathcal{D}} \leftarrow \eta_{\mathcal{D}} \nabla_{\theta_{\mathcal{D}}} \gamma(-D - GP)$ ▷ \mathcal{D} attempts to decrease output
22: $\Delta\theta_{\mathcal{F}} \leftarrow -\eta_{\mathcal{F}} \nabla_{\theta_{\mathcal{F}}} (1 - \gamma)R$ ▷ \mathcal{F} attempts to decrease R
23: $\Delta\theta_{\mathcal{R}} \leftarrow -\eta_{\mathcal{R}} \nabla_{\theta_{\mathcal{R}}} (1 - \gamma)R$ ▷ \mathcal{R} attempts to decrease output
24: $\Delta\theta_{\mathcal{G}} \leftarrow \eta_{\mathcal{G}} \nabla_{\theta_{\mathcal{G}}} (1 - \gamma)R$ ▷ \mathcal{G} attempts to increase R
25: **end while**
26: **return** \mathcal{D}, \mathcal{F} , and \mathcal{G} .
27: **end procedure**

8.2 Training details

8.2.1 Software and architecture

The experiments presented in this paper employed a DCGAN architecture (Radford et al., 2015) and were coded in Pytorch v1.3. The DCGAN is an all-convolutional network with 5 layers. The first layer above the inputs has 128 channels, which doubles every layer, except for the highest layer which has 100 channels (or 40 for MNIST). In order for the inference and generator networks to have the same architecture, the generator must use transposed convolutions where the inference uses convolutional operators. This is the standard DCGAN architecture, but where the standard discriminator is used instead as an approximate inference network

The 2d spatial dimension of the hidden layers is halved every layer upwards. For this reason the input dimension must be a factor of 2. For MNIST this requires resizing the 28x28 images to 32x32, which we performed using Pytorch's inbuilt resize transform.

Stochasticity and activations Our architecture uses ReLU activations in the inference (or discriminator) and generator networks. As a source of stochasticity, we added Gaussian noise of fixed and isotropic variance to all nodes before applying the ReLU activations. We also experimented with Laplacian-distributed noise and found similar performance.

Stochastic 'inverse' ReLU The inference network has the purpose of estimating the posterior distribution of the generative network at layer h_{i+1} that might have generated an h_i . Because the generator applies the ReLU function, any element of h_i that is 0 could have had a negative value before truncation. That is, 0 values in h_i could have been generated by quite a large subspace of h_{i+1} . To mitigate this source of mismatch between the inferred and true posteriors, we add a simple operator

to \mathcal{F} that adds negative noise to h_i where its elements are 0. We applied negative, exponentially distributed noise with initial scale 0.5 that decayed by a factor of 10 every 30 epochs.

8.2.2 Adversarial Wake-Sleep

Here we describe the training details we found to work well for Adversarial Wake-Sleep on the above architecture. After settling upon the general configuration, we fine-tuned the hyperparameters with a random search with 100 runs. As a performance criterion, we used the classification accuracy of the linear readout from the inference network (Fig. 2C). We settled on this as it was a good indicator of stable convergence that also measured an objective aspect of performance. The configuration is summarized in Table 1.

Optimization We applied the Adam optimizer with β_1 and β_2 chosen from the range $[0, 0.99]$ and $[0.5, 0.9999]$. Each network (\mathcal{F} , \mathcal{G} , and \mathcal{D}) was allowed a different learning rate η . Training was very sensitive to relative learning rates. Our final configuration used a rate of 3×10^{-4} for \mathcal{F} , 10^{-5} for \mathcal{G} , and 10^{-4} for \mathcal{D} .

Divisive normalization It was noted in Karras et al. (2017) that a source of instability in adversarial training is a battle for scale between the discriminator and generator. This can be mitigated by forcing the feature vector at any spatial location to have unit norm. After the ReLU is applied, the features (i.e. channels) at each spatial location in each layer are divided by their L_2 norm.

Minibatch standard deviation We applied another method from Karras et al. (2017), which was to calculate the standard deviation of the features in the discriminator and supply that as input in the penultimate discriminative layer. As our wake-sleep discriminator has only one hidden layer, we calculated the standard deviation of the inference/generative features and included that as input to the wake-sleep discriminator.

Regularizing h_N The generative distribution over the top-level hidden state is fixed and known: it is a multivariate standard normal distribution. We found slightly better performance when explicitly regularizing the KL divergence of the inference distribution over h_N towards the standard normal.

Prioritized replay Sensory learning is known to involve replay events triggered by the hippocampus during sleep. Inspired by this, we tested ‘replaying’ some waking states during the Sleep phase by saving the value of h_N and inserting it into the h_N otherwise sampled from the standard normal distribution. We selected the half of each batch that had the highest wake-sleep discriminator outputs, as these network states were estimated as most inference-like (‘most surprising’ samples). Overall this strategy was not necessary for good convergence but was selected by the random search.

Gradient Penalty with an L_1 norm Since our wake-sleep discriminator approximates the Wasserstein-1 distance, the gradient with respect to its inputs (the network state of \mathcal{F} and \mathcal{G}) must be 1-Lipschitz. We applied the gradient penalty GP of Gulrajani et al. (2017) and minimized the distance of the gradients from having unit norm. Whereas the typical GP minimizes the L_2 distance, we found much better performance with minimizing the L_1 norm from . Parameter searches found the proper penalty to be around $\lambda = 0.9$.

Spectral normalization in the inference network We included the option of applying spectral normalization on the inference network in our parameter searches (Miyato et al., 2018). Its usage was selected in the randomly found best configuration, but did not appear essential for stable training.

Batch normalization in the inference network The final configuration setting in the random search included batch normalization (Ioffe & Szegedy, 2015) applied to the inference network but not the generator network.

8.2.3 Doubly Adversarial Wake-Sleep

For our experiments in which the inference network was reused as a discriminator on inputs, we used the same setup but allowed hyperparameters to change. Once again, we performed a random search

Hyperparameter choices									
Algorithm	$\eta_{\mathcal{F}}$	$\eta_{\mathcal{G}}$	$\eta_{\mathcal{D}}$	$\eta_{\mathcal{R}}$	β_1	β_2	$\lambda_{\mathcal{D}}$	$\lambda_{\mathcal{F},\mathcal{R}}$	ϵ
Wake-Sleep (binary)	10^{-3}	10^{-3}	—	—	0.5	0.999	—	—	—
Adversarial Wake-Sleep	3×10^{-4}	10^{-5}	10^{-4}	—	0.6	0.999	0.9	—	0.01
Doubly Adversarial Wake-Sleep	8×10^{-4}	2×10^{-4}	10^{-5}	10^{-5}	0	0.9	0.7	7	0.01

Table 1: Hyperparameters chosen by random search. Key: η : learning rate for inference \mathcal{F} , generator \mathcal{G} , wake-sleep discriminator \mathcal{D} , and readout discriminator \mathcal{R} . β_1 and β_2 are the momentum parameters of the Adam optimizer. $\lambda_{\mathcal{D}}$ is the gradient penalty upon the wake-sleep discriminator. $\lambda_{\mathcal{F},\mathcal{R}}$ is the gradient penalty w/r/t the input images of the output of \mathcal{R} . ϵ is the initial variance of the Gaussian noise applied to activations of \mathcal{F} and \mathcal{G} .

over the parameter space and selected the configuration with the best classification accuracy from a linear SVM reading out from the top inference layer. The configuration is shown in Table 1.

Since \mathcal{F} is now also a discriminator, we are required in the WGAN formulation to apply a gradient penalty on the inputs (here, the images). We used the standard WGAN-GP penalty (Gulrajani et al., 2017). To distinguish from the gradient penalty on \mathcal{D} , we denote the strength of this penalty as $\lambda_{\mathcal{F},\mathcal{R}}$.

8.2.4 Wake-Sleep

As a comparison, we coded Wake-Sleep in a DCGAN-like architecture with continuous latent variables with ReLU activations. This is not the first paper to apply the Wake-Sleep algorithm, which is traditionally applied to stochastic binary networks, to continuous latent variables (Kingma & Welling, 2013).

Wake-Sleep trains the inference connections in the Sleep phase by maximizing at each layer i , $\log p(h_{i+1}|h_i; \mathcal{F})$, where h is a generative state. Similarly, during the Wake phase the generative connections maximize $\log p(h_i|h_{i+1}; \mathcal{G})$, where h is an inferred state. More details can be found in Hinton et al. (1995).

Stochastic Binary Convolutional Networks First, as a control, we noted that Wake-Sleep does produce digit-like images on binarized MNIST when the DCGAN architecture is a stochastic binary network (Figure 4). In a stochastic binary network, the activations and outputs are Bernoulli random variables with a probability of firing equal to a sigmoidal function of the convolved filter output. This is the original setting of the Wake-Sleep algorithm.

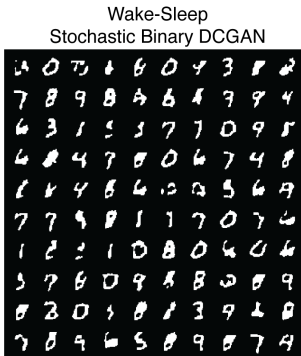


Figure 4: Binary MNIST digits generated by a stochastic binary network with convolutional filters in a DCGAN architecture, trained with the Wake-Sleep algorithm. Digits were rescaled to 32x32 to be compatible with the DCGAN architecture, then binarized by rounding. All parameters were adjusted with learning rates of 0.001 and the Adam optimizer.

ReLU Convolutional Networks We wished to compare the Wake-Sleep algorithm in our setting of continuous latent variable networks with ReLU activations and injected noise. We explored a wide parameter space. However, the Wake-Sleep algorithm was unstable for all tested configurations. We employed a random search over the space with 250 runs, plus a number of choices selected by hand. The choices of configuration included the following:

- Gaussian or Laplacian injected noise. In addition to affecting dynamics, the form of this noise affects the Wake-Sleep update rule. For Gaussian noise, $\log p(h_{i+1}|h_i; \mathcal{F})$ is the L_2 error between the generated state and the prediction of h_{i+1} by \mathcal{F} given h_i . For Laplacian noise, the log-likelihood is the L_1 error.
- The scale of the (isotropic) noise ϵ , chosen in the range $[0.1, 0.0001]$.
- The learning rate of the Adam optimizer for the inference and generative connections, which we allowed to differ. Learning rates spanned the range $[0.01, 0.00001]$.
- The β_1 and β_2 parameters of the Adam optimizer, chosen in the range $[0, 0.99]$ and $[0.5, 0.999]$.
- Spectral normalization on the inference network (Miyato et al., 2018).
- Divisive normalization on inference and generative networks, in which the channels in each layer are divided by the norm of the channels at that spatial location. This is the ‘pixelwise feature normalization’ of Karras et al. (2017).
- ReLU activation functions or SELU activations
- Dropout on the activations with $p = 0.2, 0.5, 0.8$, if applied.

All parameter configurations were unstable with the Wake-Sleep algorithm. Training produced either images of pure black, pure white, or random featureless noise.